

## Thermodynamic assessment of solid oxide fuel cell system integrated with bioethanol purification unit

W. Jamsak<sup>a</sup>, S. Assabumrungrat<sup>a,\*</sup>, P.L. Douglas<sup>b,\*\*</sup>, E. Croiset<sup>b</sup>,  
N. Laosiripojana<sup>c</sup>, R. Suwanwarangkul<sup>d</sup>, S. Charojrochkul<sup>e</sup>

<sup>a</sup> Center of Excellence in Catalysis and Catalytic Reaction Engineering, Department of Chemical Engineering, Faculty of Engineering, Chulalongkorn University, Thailand

<sup>b</sup> Department of Chemical Engineering, University of Waterloo, Canada

<sup>c</sup> The Joint Graduate School of Energy and Environment, King Mongkut's University of Technology, Thonburi, Thailand

<sup>d</sup> School of Bio-Chemical Engineering and Technology, Sirindhorn International Institute of Technology, Thammasart University, Rangsit Campus, Patum Thani 12121, Thailand

<sup>e</sup> National Metal and Materials Technology Center (MTEC), Thailand

Received 8 May 2007; received in revised form 27 August 2007; accepted 28 August 2007

Available online 7 September 2007

### Abstract

A solid oxide fuel cell system integrated with a distillation column (SOFC–DIS) has been proposed in this article. The integrated SOFC system consists of a distillation column, an EtOH/H<sub>2</sub>O heater, an air heater, an anode preheater, a reformer, an SOFC stack and an afterburner. Bioethanol with 5 mol% ethanol was purified in a distillation column to obtain a desired concentration necessary for SOFC operation. The SOFC stack was operated under isothermal conditions. The heat generated from the stack and the afterburner was supplied to the reformer and three heaters. The net remaining heat from the SOFC system ( $Q_{\text{SOFC,Net}}$ ) was then provided to the reboiler of the distillation column. The effects of fuel utilization and operating voltage on the net energy ( $Q_{\text{Net}}$ ), which equals  $Q_{\text{SOFC,Net}}$  minus the distillation energy ( $Q_{\text{D}}$ ), were examined. It was found that the system could become more energy sufficient when operating at lower fuel utilization or lower voltage but at the expense of less electricity produced. Moreover, it was found that there were some operating conditions, which yielded  $Q_{\text{Net}}$  of zero. At this point, the integrated system provides the maximum electrical power without requiring an additional heat source. The effects of ethanol concentration and ethanol recovery on the electrical performance at zero  $Q_{\text{Net}}$  for different fuel utilizations were investigated. With the appropriate operating conditions (e.g.  $C_{\text{EtOH}} = 41\%$ ,  $U_f = 80\%$  and EtOH recovery = 80%), the overall electrical efficiency and power density are 33.3% (LHV) and 0.32 W cm<sup>-2</sup>, respectively.  
© 2007 Elsevier B.V. All rights reserved.

**Keywords:** Solid oxide fuel cell; Combined process; Bioethanol; Distillation unit

### 1. Introduction

A solid oxide fuel cell is an attractive power generation system as it offers a wide range of applications, low emissions, fuel flexibility and high system efficiency. Generally, the major components of an SOFC system are preheaters, a fuel processor, a fuel cell stack and an afterburner. It is known that useful heat is always available when operating the SOFC because of the

presence of irreversibility and unreacted fuel [1]. To enhance the system efficiency, an SOFC is usually integrated with other energy devices for further utilization of excess heat to generate extra electrical power and/or hot water/steam. Nowadays, the two most promising systems are SOFC–Gas Turbine system (SOFC–GT) [2–4] and SOFC–Combined Heat and Power system (SOFC–CHP) [5–8].

For the SOFC–GT system, Palsson et al. [2] investigated a 500 kW methane-fuelled SOFC–GT system. The system consisted of preheaters, a pre-reformer, an SOFC stack, a combustor, an air compressor, a booster and an expander. Part of the anode effluent was recycled in order to supply heat and steam to the external reformer. The rest of the anode effluent was combined with the cathode effluent and burnt in the combustor. The out-

\* Corresponding author. Tel.: +662 218 6868; fax: +662 218 6877.

\*\* Corresponding author.

E-mail addresses: [Suttichai.A@chula.ac.th](mailto:Suttichai.A@chula.ac.th) (S. Assabumrungrat), [pdouglas@cape.uwaterloo.ca](mailto:pdouglas@cape.uwaterloo.ca) (P.L. Douglas).

### Nomenclature

$C_{\text{EtOH}}$	ethanol concentration (% mol)
$E$	electromotive force of a cell (V)
$E_a$	activation energy ( $\text{J mol}^{-1}$ )
$F$	Faraday constant ( $\text{C mol}^{-1}$ )
$i$	current density ( $\text{A cm}^{-2}$ )
$I$	current (A)
$\text{LHV}_{\text{EtOH}}$	lower heating value of ethanol ( $\text{J mol}^{-1}$ )
$n_{\text{EtOH}}$	total ethanol flow rate fed to the distillation column ( $\text{mol s}^{-1}$ )
$p_i$	partial pressure of component $i$ (kPa)
$P$	pressure (kPa)
$P_{\text{den}}$	power density ( $\text{A cm}^{-2}$ )
$Q_1$	the energy required for Preheater 1 (kW)
$Q_2$	the energy required for Preheater 2 (kW)
$Q_3$	the energy required for Preheater 3 (kW)
$Q_4$	the energy required for a reformer (kW)
$Q_5$	the exothermic heat released from an SOFC stack (kW)
$Q_6$	the energy involved the combustion of exhausted gases and cooled to the exit temperature (kW)
$Q_{\text{Con}}$	condenser duty (kW)
$Q_{\text{D}}$	reboiler duty (kW)
$Q_{\text{Net}}$	net useful heat (kW)
$Q_{\text{SOFC,Net}}$	net exothermic from SOFC (kW)
$r$	area specific resistance ( $\Omega \text{ cm}^2$ )
$r_{\text{act}}$	activation polarization area specific resistance ( $\Omega \text{ cm}^2$ )
$r_{\text{ohm}}$	ohmic polarization area specific resistance ( $\Omega \text{ cm}^2$ )
$r_{\text{H}_2,\text{cons}}$	rate of hydrogen consumed by the electrochemical reaction ( $\text{mol s}^{-1}$ )
$R$	gas constant ( $\text{J mol}^{-1} \text{ K}^{-1}$ )
$T_{\text{SOFC}}$	SOFC temperature (K)
$T_{\text{RF}}$	reforming temperature (K)
$U_{\text{f}}$	fuel utilization (%)
$V$	operating voltage (V)
$W_e$	electrical power (kW)
<i>Greek letters</i>	
$\eta_{\text{elec,ov}}$	overall electrical efficiency (%)
$\rho$	resistivity ( $\Omega \text{ cm}$ )

### Subscripts

a	anode
c	cathode

$\text{CO}_2$  capture plant. The desulfurizer unit was also implemented in the SOFC system. The  $\text{CO}_2$  capture plant consisted of a condenser, an absorber and a regenerator. Two SOFC stacks were employed in this study. The reformed gas was split between the two stacks and fed to the anode sides in parallel. The obtained electrical efficiency of the SOFC–GT system integrated with the  $\text{CO}_2$  capture plant reached above 60%. Inui et al. [4] investigated SOFC–GTs with  $\text{CO}_2$  recovery systems. Two new  $\text{CO}_2$  recovery systems were proposed as a bottoming cycle, i.e. (1)  $\text{CO}_2$  recycle system and (2) water vapor injection system. The results showed that the former system achieved an overall efficiency of 70.88% (LHV) while the latter system yielded 72.13%.

For the SOFC–CHP system, Chan et al. [5] studied a methane-fuelled SOFC system and compared its efficiency with that of a hydrogen-fuelled system. The system consisted of a vaporizer, preheaters, a pre-reformer, an SOFC stack and an afterburner. The unreacted fuel was burnt in the afterburner and the heat from the afterburner was supplied to the reformer, vaporizer, steam boiler and preheaters. Some heat from the SOFC stack was used for the steam boiler. The results indicated that the efficiency of the methane-fuelled system was higher than that of the hydrogen-fuelled system. Fontell et al. [6] examined a methane-fuelled SOFC combined with a desulfurizer unit, a power conversion unit and system controllers. The system configuration was different from Chan's work [5] as the anode effluent was re-circulated for preheating the reformed gas before being split into two streams: one was mixed with the desulfurized stream and the other was fed to the combustor. The results revealed that the system efficiency achieved was around 85%. Zhang et al. [7] also examined an SOFC fuelled with methane. The equipment setting was almost similar to that in Fontell's work [6]; however, no desulfurizer, power conversion and controllers were included. In addition, the anode effluent was also split into two streams: one for combustion and the other for anode re-circulation. No anode effluent was used for preheating the anode inlet. An electrical efficiency of 52% was obtained for the desired power of 120 kW. Omosun et al. [8] studied an SOFC fuelled by product gas from gasified biomass. The system consisted of a gasifier, separation units (i.e. cyclone and filter), a fuel cell stack and a combustor. The study focused on a performance comparison between cold and hot processes. The major differences between those processes were the gasification and clean-up processes. The hot process used a fluidized bed gasifier and a ceramic filter whereas the cold process used a fixed-bed gasifier and a wet precipitator. For a heat recovery, both anode and cathode effluents were re-circulated and mixed with the incoming streams. The results showed that the hot process yielded higher electrical and system efficiencies than the cold process. However, the cost of the hot process was higher than that of the cold process.

Among the many possible fuels for SOFC, ethanol is an attractive green fuel as it can be derived from renewable resources and it is safe and easy for storage and handling [9]. The group of Tsiakaras has been particularly active in investigating the ethanol-fuelled SOFCs [10–12]. They compared the theoretical SOFC performances for different ethanol reforming reactions (steam reforming,  $\text{CO}_2$  reforming and par-

let stream from the combustor was then delivered to the gas turbine for generating additional electrical power whereas the exhaust gas from the gas turbine was used for preheating the feeds. The influences of operating parameters such as pressure, air flow rate, fuel flow rate and air inlet temperature on the system performance were analyzed. Fredriksson Möller et al. [3] studied a methane-fuelled SOFC–GT system integrated with a

tial oxidation) [10]. It was reported that the products from steam reforming yielded the highest maximum efficiency when  $T < 950$  and  $> 1100$  K whereas those from the  $\text{CO}_2$  reforming was more preferable at the intermediate temperatures. For the partial oxidation, its efficiency was 20% less than the other cases. An energy–exergy analysis was also employed to examine the system comprising an external steam reformer, an SOFC stack, an afterburner, two preheaters, a water vaporizer and a mixer [11,12]. No anode and cathode recycles were considered. The heat from the combustor was provided to the preheaters, the vaporizer and the reformer. An optimization of the combustor was performed by matching appropriate reforming temperature and fuel utilization. Moreover, the minimization of SOFC loss was examined by searching for suitable reforming and air preheating temperatures. It should be noted from all studies related to SOFCs fuelled by ethanol that pure ethanol was usually mixed with water in order to obtain a desired ethanol concentration before being fed into the reformer. From an energy point of view, this might not be an efficient strategy as unnecessary energy is consumed to purify bioethanol to a needless high concentration ethanol, which is subsequently mixed with water and fed to the reformer.

In this work, it was proposed to integrate the SOFC with an ethanol purification unit. The ethanol was purified to a desired concentration using a distillation column whose required energy can be directly supplied from the excessive heat from the SOFC system. It was expected that by carefully selecting suitable operating conditions, the integrated system could be operated without any requirement of additional energy sources apart from the bioethanol feed. The influences of operating parameters including ethanol concentration, ethanol recovery, fuel utilization and voltage on electrical performance and net energy of the integrated system ( $Q_{\text{Net}}$ ) were investigated.

## 2. SOFC system modelling

Fig. 1 shows the proposed SOFC system integrated with a distillation column (SOFC–DIS). The SOFC system consisted of three heat exchangers (for preheating feeds), a reformer and an afterburner. The distillation column was integrated with the SOFC system to purify bioethanol to desired levels of ethanol concentration and recovery. Generally, the ethanol concentration from a fermentation process is in the range of 1–7 mol% [13–16]. In this work, the value of 5 mol% was selected as a representative of bioethanol. Aspen Plus<sup>TM</sup> and the Radfrac rigorous

equilibrium stage distillation module were used for simulating the distillation column. A total condenser and a kettle boiler were employed. The bioethanol feed was introduced to the stage above the reboiler. The minimum reboiler heat duty, which could be obtained by adjusting the number of stages and reflux ratio, was used in the present study of the SOFC–DIS system.

The distillate leaving the distillation column was heated up to the reforming temperature ( $T_{\text{RF}}$ ) by Heater 1 (here  $T_{\text{RF}} = 1023$  K), and fed to the external reformer, which was assumed to operate isothermally. It should be noted that considering such high reforming temperature, negligible extent of ethanol was present in the reformed gas. The reformed gas was then heated up to the SOFC temperature ( $T_{\text{SOFC}}$ ) by Heater 2 and introduced to the anode chamber of the SOFC stack. The SOFC stack was also assumed to operate isothermally ( $T_{\text{SOFC}} = 1200$  K). Excess air (380%) preheated by Heater 3 was fed to the cathode chamber. The equations describing the electrochemical model are as follows:

$$V = E - i(r_{\text{ohm}} + r_{\text{act}}) \quad (1)$$

$$E = \frac{RT}{4F} \ln \frac{p_{\text{O}_2,\text{c}}}{p_{\text{O}_2,\text{a}}} \quad (2)$$

$$r_{\text{act,c}} = \left[ \frac{4F}{RT} k(p_{\text{O}_2,\text{c}})^m \exp\left(-\frac{E_{\text{a,c}}}{RT}\right) \right]^{-1} \quad (3)$$

$$r_{\text{act,a}} = \left[ \frac{2F}{RT} k(p_{\text{H}_2,\text{a}})^m \exp\left(-\frac{E_{\text{a,a}}}{RT}\right) \right]^{-1} \quad (4)$$

$$r_{\text{ohm},j} = \rho_j \delta_j \quad (5)$$

$$\rho_j = \alpha_j \exp\left(\frac{\beta_j}{T}\right) \quad (6)$$

$$P_{\text{den}} = iV \quad (7)$$

$$I = r_{\text{H}_2,\text{cons}} \times 2F \quad (8)$$

$$r_{\text{H}_2,\text{cons}} = r_{\text{H}_2,\text{in,equiv.}} \times U_f \quad (9)$$

$$r_{\text{H}_2,\text{in,equiv.}} = 6 \times r_{\text{EtOH,d}} \quad (10)$$

$$A = \frac{I}{i} \quad (11)$$

$$W_e = IV \quad (12)$$

where  $E$  is the electromotive force (EMF),  $V$  the operating voltage,  $i$  the current density,  $I$  the overall current,  $R$  the gas constant,  $T$  the SOFC temperature,  $F$  the Faraday's constant,  $r_{\text{act}}$  the activation resistance,  $E_{\text{a,a}}$  and  $E_{\text{a,c}}$  the activation energies at anode and cathode, respectively,  $p_{\text{O}_2,\text{c}}$  and  $p_{\text{H}_2,\text{a}}$  the mole fractions of oxygen in the cathode chamber and hydrogen in the anode chamber, respectively,  $r_{\text{ohm}}$  the ohmic resistance,  $\rho_j$  the resistivity of material  $j$ ,  $\alpha_j$  and  $\beta_j$  the constants specific to material  $j$ ,  $r_{\text{H}_2,\text{cons}}$  the molar flow rate of hydrogen consumed in the electrochemical reaction,  $r_{\text{H}_2,\text{in,equiv.}}$  the maximum hydrogen molar flow rate coming into the anode chamber ( $6 \times$  that of ethanol flow rate),  $r_{\text{EtOH,d}}$  the ethanol flow rate in the distillate fed into the SOFC system,  $A$  the total active area of SOFC stack,  $W_e$  the electrical power,  $P_{\text{den}}$  the power density,  $\text{LHV}_{\text{EtOH}}$  the low heating value

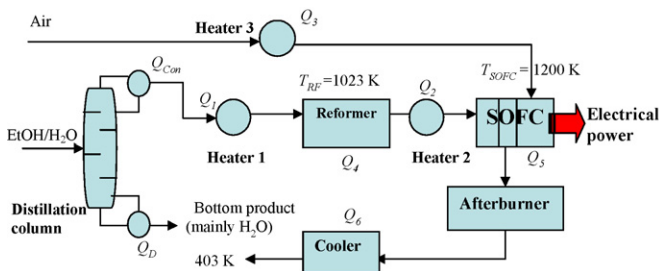


Fig. 1. Schematic diagram of SOFC system integrated with a distillation column (SOFC–DIS).

Table 1  
Parameters for activation loss [17]

$r_{\text{act}}$ ( $\Omega \text{ cm}^2$ )	$k$ ( $\times 10^{-13} \text{ A cm}^2$ )	$E_a$ ( $\text{kJ mol}^{-1} \text{ K}^{-1}$ )	$m$ (–)
$r_{\text{act,c}}$	14.9	160	0.25
$r_{\text{act,a}}$	0.213	110	0.25

of ethanol. The parameters used for calculating the ohmic and activation overpotentials are listed in Tables 1 and 2.

It should be noted that the SOFC cell was based on the tubular configuration [5]. Concerning the activation losses, the Achenbach's semi-empirical correlation [17] was used to predict the activation overpotentials for the anode and cathode. Hernandez-Pacheco et al. [18] compared the values from the Achenbach's correlation and the Butler–Volmer equation and found that the Achenbach's correlation gave reliable results for temperatures between 1173 and 1273 K. The operating temperature of 1200 K in this study was within the reliable range of the Achenbach's correlations. For calculating SOFC performance, a concentration polarization loss could be omitted when an SOFC does not operate at high current density. The concentration losses can be estimated by using an equation given in Ref. [19]. A concentration loss of 0.03 V was thus estimated at the current densities around  $0.6 \text{ A cm}^{-2}$ . This is why the concentration polarization was neglected. Details on the calculations of composition and EMF distributions within the SOFC stack were given in our previous works [20,21]. Note that the flow rate of ethanol is kept constant for all conditions; therefore, the active area of the SOFC stack were changed when the voltage and fuel utilization changed. The appropriate size of SOFC stack was not investigated in this work.

The effluent from the anode and the cathode was burnt in the afterburner. Assuming that the combusted gas was discharged to the environment at 403 K, the useful heat remaining in the exhaust stream could be calculated. The useful heat is used to supply the energy to the energy-demanding units in the system (such as reboiler, heaters and reformer). It should be noted that the temperature of the exhaust gas to the environment should be higher than the dew point of water to avoid water condensation, which may cause corrosion due to acidic condensate in pipelines. For efficient heat utilization in the system, the exothermic heat from the SOFC stack ( $Q_5$ ) and the afterburner ( $Q_6$ ) were supplied to the energy-consuming units of the SOFC system (the heaters ( $Q_1$ ,  $Q_2$  and  $Q_3$ ) and the reformer ( $Q_4$ )). The net useful heat from the SOFC system ( $Q_{\text{SOFC,Net}}$ ) was defined as the difference between the exothermic heat (SOFC stack and afterburner) and the endothermic heat (preheaters and reformer) of

Table 2  
Parameters of ohmic loss in SOFC cell components [5]

Materials	Parameters		Thickness ( $\mu\text{m}$ )
	$\alpha$ ( $\Omega \text{ cm}$ )	$\beta$ (K)	
Anode (40% Ni/YSZ cermet)	$2.98 \times 10^{-5}$	–1392	150
Cathode (Sr-doped LaMnO <sub>3</sub> : LSM)	$8.11 \times 10^{-5}$	600	2000
Electrolyte (Y <sub>2</sub> O <sub>3</sub> -doped ZrO <sub>2</sub> : YSZ)	$2.94 \times 10^{-5}$	10350	40
Interconnect (Mg-doped LaCrO <sub>3</sub> )	$1.256 \times 10^{-3}$	4690	100

the SOFC system. Generally,  $Q_{\text{SOFC,Net}}$  was positive and could be further utilized for the distillation column. The net useful heat ( $Q_{\text{Net}}$ ) of the SOFC–DIS system was calculated as the difference between the net useful heat of the SOFC system ( $Q_{\text{SOFC,Net}}$ ) and the distillation energy ( $Q_D$ ), in this case the reboiler heat duty. For energy calculation, the heat involved in each unit can be calculated using a conventional energy balance. The overall electrical efficiency was calculated as follows:

$$\eta_{\text{elec,ov}} = \frac{IV}{n_{\text{EtOH}} \times \text{LHV}_{\text{EtOH}}} \quad \text{when } Q_{\text{Net}} \geq 0 \quad (13)$$

$$\eta_{\text{elec,ov}} = \frac{IV}{(n_{\text{EtOH}} \times \text{LHV}_{\text{EtOH}}) - Q_{\text{Net}}} \quad \text{when } Q_{\text{Net}} \leq 0 \quad (14)$$

where  $n_{\text{EtOH}}$  represents the total ethanol flow rate fed to the distillation column. For  $Q_{\text{Net}} \leq 0$ , the SOFC–DIS system required more energy from an external heat source. To calculate the actual overall electrical efficiency, the energy required from the external heat source should be taken into account.

### 3. Results and discussion

#### 3.1. Effect of ethanol concentration on SOFC performance and energy requirement in the distillation column

It is impractical to directly reform bioethanol to generate a fuel gas for an SOFC stack due to the high water content [22]. Fig. 2 shows the performance curves of SOFCs fed by various reformed gases from the reforming of ethanol at different concentrations. The SOFC operated at a  $T_{\text{SOFC}}$  of 1200 K with a fuel utilization ( $U_f$ ) of 80%. From Fig. 2 it is clear that the power density, cell voltage and electrical efficiency increase with increasing ethanol concentration. This implies that the SOFC stacks perform better when a distillation column is integrated with the SOFC system to purify the bioethanol. However, in practice, the maximum ethanol concentration should be kept below the range of carbon formation to avoid deactivation of the reforming catalyst and anode of the SOFC cell. For example, at  $T_{\text{RF}} = 1023 \text{ K}$ , the boundary of carbon formation was at 41 mol% [20].

Although it is advantageous to use ethanol at high concentrations for the SOFC system, an additional energy is required to concentrate the bioethanol. Fig. 3 shows the minimum reboiler and condenser heat duties as a function of ethanol purity and recovery. It is clear that more energy is required when the distillation column is operated to achieve higher ethanol concentration and recovery. The reboiler and condenser heat duties increase dramatically at low ethanol purity and rises steadily at the higher ethanol purity. This is due to a narrow vapor–liquid equilibrium gap for ethanol–water mixture at low ethanol purity and a wider vapor–liquid gap at higher purity.

#### 3.2. Performance of the SOFC system integrated with a distillation column (SOFC–DIS) at base case conditions

Fig. 4 indicates the temperature and energy requirement for all important units in the SOFC–DIS system operating at base

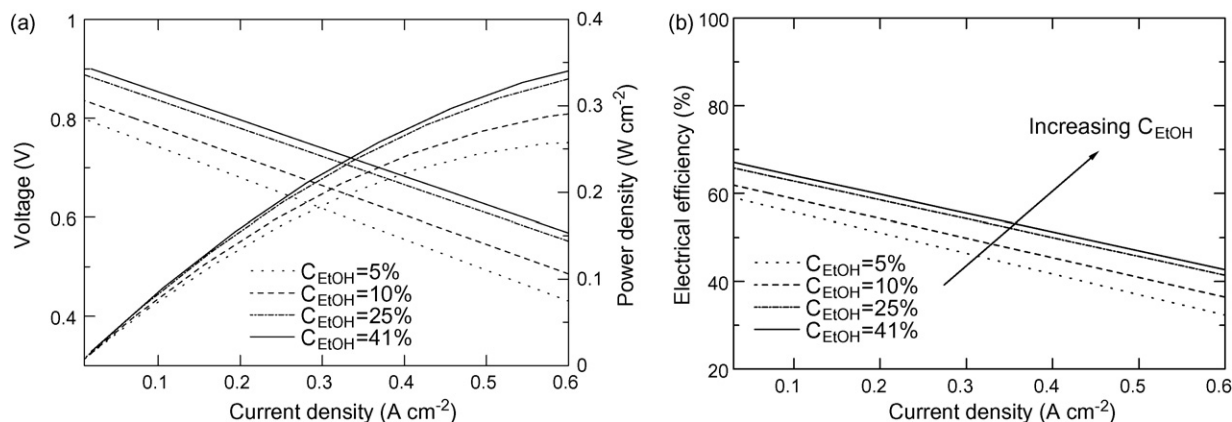


Fig. 2. Effect of ethanol concentration on SOFC performance: (a) voltage and power density and (b) electrical efficiency ( $U_f = 80\%$  and  $P = 101.3$  kPa).

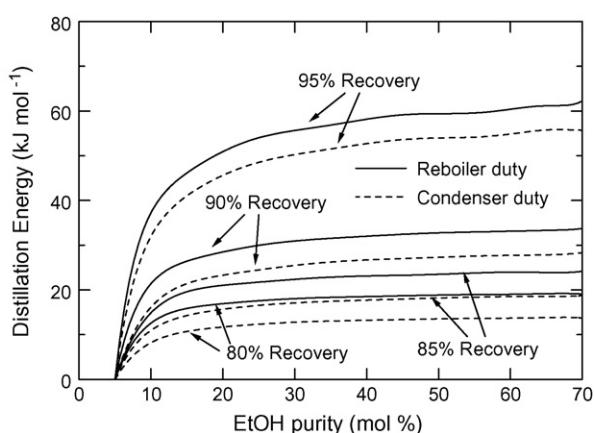


Fig. 3. Effect of ethanol concentration and ethanol recovery on distillation energy.

case conditions, i.e.  $C_{EtOH} = 25$  mol%, EtOH recovery = 80%, cell operating voltage = 0.7 V and  $U_f = 80\%$ . An electrical power ( $W_e$ ) of 218.77 kW with an overall electrical efficiency (based on LHV) of 37.72% was achieved. The net useful heat of the SOFC system ( $Q_{SOFC,Net}$ ) and the heat required for the distillation column ( $Q_D$ ) are 88.36 and 149.11 kW, respectively. In this case, although  $Q_{SOFC,Net}$  can be used for supplying heat to the reboiler directly, it is obvious that the amount of  $Q_{SOFC,Net}$  is not enough for the required  $Q_D$  under these base conditions. The conditions and the performance of SOFC–DIS system (power, power density,  $Q_{Net}$ ) at the base case are presented in Table 3. However, by carefully adjusting the operating conditions such

Table 3

Summary of operating conditions and the performance of SOFC for the base case

Parameter	Value/quality
Bioethanol flow rate ( $\text{mol s}^{-1}$ )	8.42
Ethanol recovery (%)	80
Fuel option	Bioethanol with 5 mol% EtOH in water
Reforming temperature (K)	1023
SOFC temperature (K)	1200
Fuel utilization (%)	80
Voltage (V)	0.7
Power (kW)	218.77
$Q_{Net}$ (kW)	−60.75
Overall electrical efficiency (%)	37.72

as operating voltage, fuel utilization, ethanol concentration and recovery, excess heat from the SOFC system can be increased to satisfy the energy requirements of the reboiler in the distillation column. A proper adjustment of these operating conditions for the system to be self-sufficient ( $Q_{Net} = Q_{SOFC,Net} - Q_D = 0$ ) is the subject of the subsequent sections.

### 3.3. Effects of operating parameters

#### 3.3.1. Effects of SOFC operating voltage and fuel utilization

Fig. 5 represents the effect of operating voltage and fuel utilization on the overall efficiency and electrical power,  $W_e$ , (Fig. 5a), net useful heat,  $Q_{Net}$ , (Fig. 5b) and power density (Fig. 5c). As mentioned earlier,  $Q_{Net}$  is  $Q_{SOFC,Net}$  subtracted by  $Q_D$ . Therefore, the value of  $Q_{Net}$  can be positive, zero or negative. A positive value of  $Q_{Net}$  indicates that some extra heat is left from the overall SOFC–DIS system. For the case where  $Q_{Net}$  is negative,  $Q_{SOFC,Net}$  is not enough to supply all the required heat to the distillation column; therefore, an external heat source is required. At the point where  $Q_{Net}$  is equal to zero,  $Q_{SOFC,Net}$  satisfies exactly the reboiler demand. Consequently, this condition offers the maximum electrical power for the SOFC–DIS system without requiring an external heat source. From Fig. 5b it can be seen that higher  $Q_{Net}$  (i.e. the system becomes more energy sufficient) can be obtained when the SOFC–DIS system operates

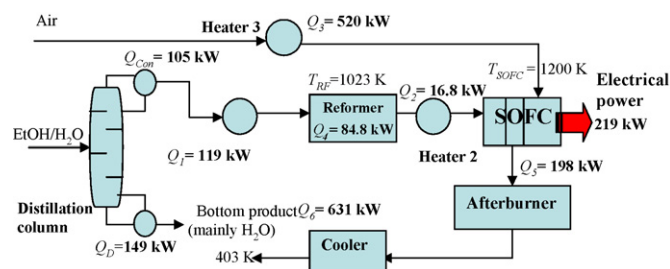


Fig. 4. Energy and temperature for various units in the SOFC–DIS system (EtOH recovery = 80%,  $C_{EtOH} = 25$  mol%,  $U_f = 80\%$ , and  $P = 101.3$  kPa).

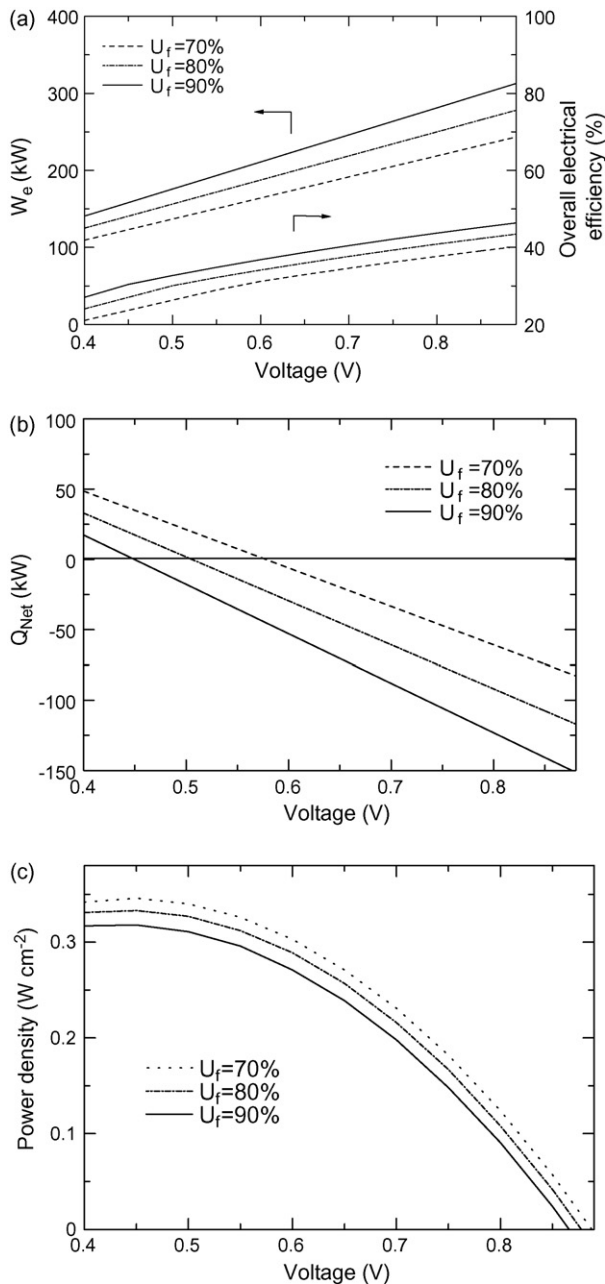


Fig. 5. Effect of operating voltage and  $U_f$  on SOFC–DIS performance: (a)  $W_e$  and overall efficiency, (b)  $Q_{Net}$  and (c) power density (EtOH recovery = 80%,  $C_{EtOH} = 25 \text{ mol}\%$ , and  $P = 101.3 \text{ kPa}$ ).

at lower voltage and/or lower fuel utilization. For lower voltage operation, the difference between the theoretical voltage and the actual one is large and results in higher heat losses emitted from the SOFC stack and therefore,  $Q_{Net}$  increases. For operation at a lower fuel utilization, more unreacted fuel exiting the SOFC stack is burnt in the afterburner. This leads to higher combustion energy and, as a result, higher  $Q_{Net}$ . However, lower electrical power and overall efficiency are obtained at higher  $Q_{Net}$ . There is an appropriate voltage for which  $Q_{Net} = 0$  for  $U_f$  ranging from 70 to 90% (at  $C_{EtOH} = 25\%$  and EtOH recovery = 80%). The corresponding voltages are 0.58, 0.51 and 0.45 V, for  $U_f = 70, 80$  and 90%, respectively. Operation at higher fuel utilization requires

lower operating voltage for generating more heat from the stack to compensate for the heat required in the overall system.

Another important SOFC performance indicator, which should be of concern, is the power density. The effects of voltage and fuel utilization on power density are shown in Fig. 5(c). An operation at low voltage is of no practical value (hence, not shown in Fig. 5). However, at high voltage Fig. 5c shows a rapid decrease in power density, resulting in larger (increased area) and more expensive SOFC stacks. Fig. 5b and c also indicate that for voltages corresponding to  $Q_{Net}$  equal to zero, the power densities are equal to 0.31, 0.33 and 0.32  $\text{W cm}^{-2}$  for  $U_f = 70, 80$  and 90%, respectively, which also corresponds to an overall electrical efficiency of 30.3% for all fuel utilizations. The fuel utilization factor (at least in the range of 70–90%) has thus no notable influence on the overall electrical efficiency and power density when  $Q_{Net}$  is kept at zero (at constant ethanol concentration).

In summary, the SOFC–DIS system can be made self-sufficient by adjusting the fuel utilization and operating voltage. However, it should be noted that a number of operating parameters must be carefully examined. An operation of SOFC at too low voltage may result in a significant reduction in power density. Moreover, the excessive heat generated in the stack will directly damage the thermophysical property of the SOFC cell components and raises the issue of how to remove this high amount of heat from the stack. It is recommended that adjusting fuel utilization is a better option to control  $Q_{SOFC,Net}$ . Also, for practical operation, the electrical power, overall efficiency and power density should be acceptably high.

### 3.3.2. Effect of ethanol concentration

From the previous section, it was found that an adjustment of voltage and fuel utilization can render the system self-sufficient. However,  $Q_{Net}$  also depends on the amount of required distillation energy ( $Q_D$ ), which is strongly influenced by ethanol concentration ( $C_{EtOH}$ ) and ethanol recovery (Fig. 3). In this section, the effect of ethanol concentration on electrical performance ( $W_e$ , overall efficiency, and corresponding voltage and power density) at conditions for which  $Q_{Net} = 0$  is investigated. The ethanol recovery was kept at 80%. The results shown in Fig. 6(a) indicate that, for ethanol concentrations between 15 and 41%,  $W_e$ , and overall efficiency increase with increasing ethanol concentration, independent of the fuel utilization ( $U_f = 70\text{--}80\%$ ). We know that increasing ethanol concentration is beneficial in terms of power produced, but is detrimental in terms of energy demand in the column reboiler (see Fig. 3). Fig. 6a illustrates the fact that, for ethanol concentrations between 15 and 41%, the benefit of increasing ethanol concentration is more important than the negative effect of increased reboiler duty. This could be explained by the relatively gentle increase in reboiler duty for ethanol concentrations greater than 15%, as seen in Fig. 3. The effect of fuel utilization on SOFC performance when  $Q_{Net}$  equals zero is also presented in Fig. 6(b). It can be seen that the SOFC would run at lower voltage for an operation at higher fuel utilization. This result is in good agreement with the results described earlier. It can be seen that the operating voltage is around 0.6 and 0.5 V at  $U_f = 70$  and 80%,

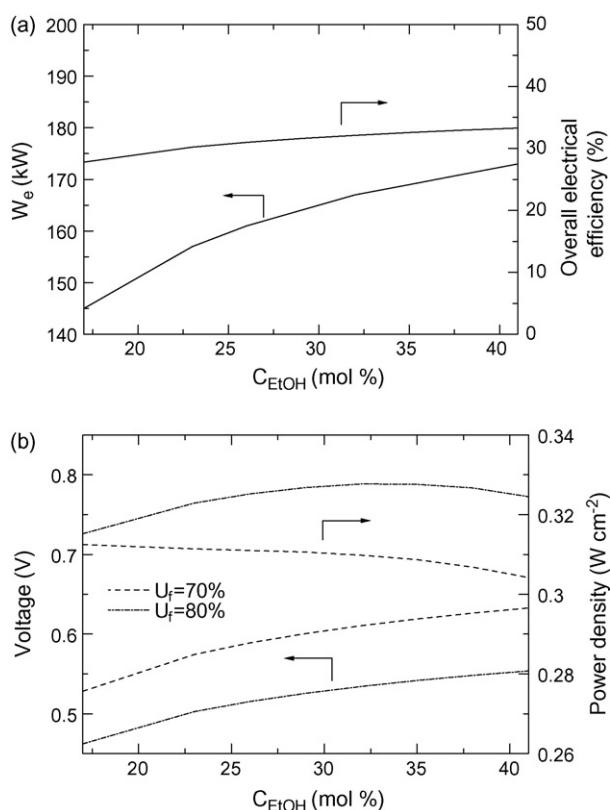


Fig. 6. Effect of ethanol concentration on SOFC–DIS performance for various  $U_f$  when  $Q_{Net} = 0$ : (a)  $W_e$  and overall efficiency and (b) corresponding voltage and power density (EtOH recovery = 80%, and  $P = 101.3$  kPa).

respectively. Fig. 6(b) also presents the effect of ethanol concentration on power density. For  $U_f = 80\%$ , the power density slightly increases when operated at higher  $C_{EtOH}$  whereas the opposite is true for  $U_f = 70\%$ . As expected, the power density is consistently higher at  $U_f = 80\%$  than at 70%.

In summary, Fig. 6 indicates that, when keeping  $Q_{Net}$  equals to zero, better overall performance (higher overall electrical efficiency, higher power density) is achieved when operating at higher fuel utilization factor (e.g. 80%) and at the highest possible ethanol concentration (i.e. 41%). At these conditions, the overall efficiency reaches 33.3% and the power density  $0.32\ W\ cm^{-2}$  (corresponding to a voltage of 0.55 V and current density of  $0.58\ A\ cm^{-2}$ ). It should be noted that in this study the SOFC cell is based on the tubular configuration. In a practical operation, a planar SOFC with higher current densities may be an attractive choice.

### 3.3.3. Effect of ethanol recovery

As mentioned earlier, an ethanol recovery is an important parameter affecting  $Q_D$  and the overall energy within the system. Fig. 7(a) presents the effect of ethanol recovery on  $W_e$  and overall efficiency at different ethanol concentrations for  $Q_{Net} = 0$ . Higher  $W_e$  and overall efficiency are obtained when increasing the ethanol recovery up to 80%; however, the performance significantly decreases at ethanol recoveries greater than 80%. This is because of the competition between an increase of current and a decrease of operating voltage at that point. By increasing the

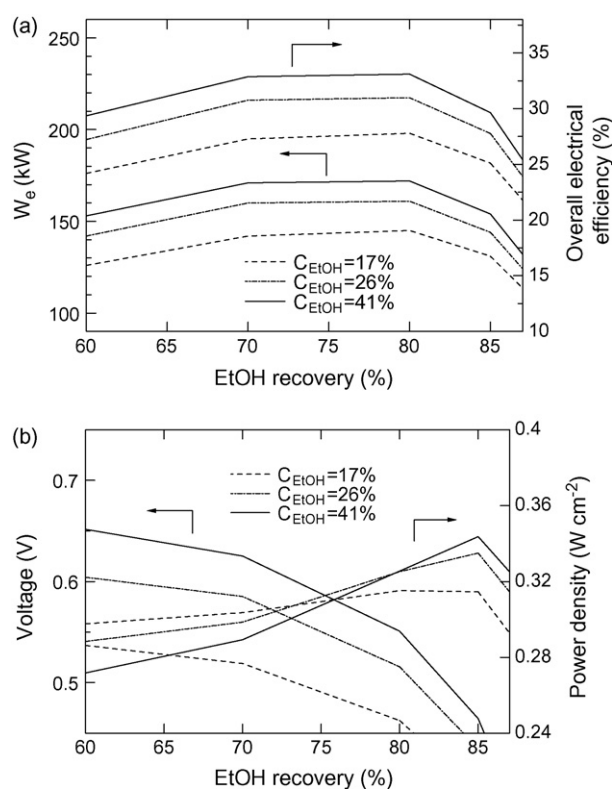


Fig. 7. Effect of ethanol recovery on SOFC–DIS performance when  $Q_{Net} = 0$  at different  $C_{EtOH}$ : (a)  $W_e$  and overall efficiency, and (b) corresponding voltage and power density ( $U_f = 80\%$  and  $P = 101.3$  kPa).

ethanol recovery, this effect also increases the current at the same fuel utilization while the operating voltage is also dependent on the required  $Q_D$ . It can be seen that at lower ethanol recovery, the required operating voltage is slightly changed due to a small change in  $Q_D$ . Therefore, the electrical power becomes higher because of the increase in current. However, at high ethanol recovery,  $Q_D$  is dramatically increased and causes a sudden drop in voltage as shown in Fig. 7(b). This results in a decrease in electrical power. The corresponding voltage and power density at different EtOH recovery is also shown in Fig. 7(b). It can be seen that an increase of ethanol recovery still requires lower voltage. The SOFC–DIS system still needs some energy from the SOFC stack to compensate for the higher demand in  $Q_D$ . This is different from the results in Fig. 6(b), which shows that lower voltage is not required because the SOFC–DIS system gain some benefits from the less preheating energy for EtOH/ $H_2O$  mixture. For the effect of ethanol recovery, more ethanol and water are fed to the SOFC–DIS system when operated at higher ethanol recovery. More energy is therefore required for the reformer and EtOH/ $H_2O$  preheater. The SOFC stack has to be operated at lower voltages to compensate for the heat, which results in a decrease in voltage as shown in Fig. 7(b). Moreover, it was found that at higher EtOH recovery, a higher power density is obtained.

From the above studies, it is possible to operate the SOFC–DIS system in an energy sufficient mode. The obtained efficiency and power density of SOFC–DIS system are 33.3% and  $0.32\ W\ cm^{-2}$  at  $C_{EtOH} = 41\%$ ,  $U_f = 80\%$  and ethanol recov-

ery = 80%. The reboiler heat duty is the limit in achieving a higher performance because the SOFC–DIS has to be operated under inferior conditions in order to provide the required heat to the distillation column. Moreover, a large amount of heat (105 kW) was emitted from the SOFC–DIS at the condenser. The management of this condenser duty could be used to enhance the SOFC–DIS performance and allow the SOFC to operate at more optimal conditions. It is expected that the performance of SOFC–DIS could be further improved.

#### 4. Conclusions

An SOFC system integrated with a distillation column (SOFC–DIS) was studied. Bioethanol was used as a feed stream for the SOFC–DIS system. The influence of operating parameters (EtOH concentration, EtOH recovery, cell operating voltage and fuel utilization) on electrical performance (e.g. electrical power, overall efficiency and power density) and thermal energy involved in the SOFC system (e.g. reboiler heat duty and the net useful heat) was presented. The study showed that it is possible to operate the SOFC–DIS system in an energy self-sufficient mode by adjusting the operating voltage and/or fuel utilization. The effect of ethanol concentration (17–41 mol%) and ethanol recovery at the energy-sufficient point ( $Q_{\text{Net}} = 0$ ) was presented. It was found that higher ethanol concentration yielded higher electrical power (for  $C_{\text{EtOH}}$  in the range of 15–17%), higher overall electrical efficiency and acceptably high power density. For the effect of ethanol recovery, there is an optimum ethanol recovery at 80%, which yielded the optimum electrical power and overall electrical efficiency. Higher power densities can be obtained when operating at higher ethanol recoveries. In brief, this thermodynamic study of the SOFC–DIS system showed the potential of the system when operated without external heat sources. However, the obtained performance of the SOFC–DIS system was quite low (0.32 W cm<sup>-2</sup>, 173.07 kW, 33.3% overall efficiency based on total ethanol flow rate fed to SOFC–DIS system at  $U_f = 80\%$ , EtOH recovery = 80% and  $C_{\text{EtOH}} = 41\%$ ). It was found that the reboiler heat duty was the limit of the SOFC–DIS system. Moreover, a huge amount of heat was lost at the condenser. To improve the performance of the SOFC–DIS system, it is recommended that (1) the heat emitted at a condenser should be utilized for other purposes and (2) another purifying pro-

cess (e.g. membranes) which consumes less energy should be investigated.

#### Acknowledgements

The support from the Thailand Research Fund, Commission of Higher Education and National Metal and Materials Technology Center (MTEC) are gratefully acknowledged.

#### References

- [1] EG&G Service Parsons Inc., Fuel Cell Handbook, 5th ed., Science Applications International Corporation, Morgantown, WV, 2000, pp. 234.
- [2] J. Pálsson, A. Selimovic, L. Sjunnesson, J. Power Sources 86 (2000) 442–448.
- [3] B. Fredriksson Möller, J. Arriagada, M. Assadi, I. Potts, J. Power Sources 131 (2004) 320–326.
- [4] Y. Inui, T. Matsumae, H. Koga, K. Nishiura, Energy Convers. Manage. 46 (2005) 1837–1847.
- [5] S.H. Chan, C.F. Low, O.L. Ding, J. Power Sources 103 (2002) 188–200.
- [6] E. Fontell, T. Kivisaari, N. Christiansen, J.B. Hansen, J. Pálsson, J. Power Sources 131 (2004) 49–56.
- [7] W. Zhang, E. Croiset, P.L. Douglas, M.W. Fowler, E. Entchev, Energy Convers. Manage. 46 (2005) 181–196.
- [8] A.O. Omosun, A. Bauen, N.P. Brandon, C.S. Adjiman, D. Hart, J. Power Sources 131 (2004) 96–106.
- [9] G. Maggio, S. Freni, S. Cavallar, J. Power Sources 74 (1998) 17–23.
- [10] P. Tsiakaras, A. Demin, J. Power Sources 102 (2001) 210–217.
- [11] S. Douvartzides, F.A. Coutelieris, P.E. Tsiakaras, J. Power Sources 114 (2003) 203–212.
- [12] S. Douvartzides, F. Coutelieris, P. Tsiakaras, J. Power Sources 131 (2004) 224–230.
- [13] D.J. Shell, C.J. Riley, N. Dowe, J. Farmer, K.N. Ibson, M.F. Ruth, S.T. Toon, R.E. Lumpkin, Bioresour. Technol. 91 (2004) 179–188.
- [14] C.A. Cardona Alzate, O.J. Sanchez Toro, Energy 31 (2006) 2447–2459.
- [15] P.L. Roger, K.J. Lee, D.E. Tribe, Process Biochem. (1980) 7–11.
- [16] S.E. Buchholz, M.M. Dooley, D.E. Eveleigh, Trends Biotechnol. 5 (1987) 199–204.
- [17] E. Achenbach, J. Power Sources 49 (1994) 333–348.
- [18] E. Hernandez-Pachenco, D. Singh, P.N. Hutton, N. Patel, M.D. Mann, J. Power Sources 138 (2004) 174–186.
- [19] M.C. Williams, J.P. Starkey, S.C. Singhal, J. Power Sources 131 (2004) 79–85.
- [20] S. Assabumrungrat, V. Pavarajarn, S. Charojrochkul, N. Laosiripojana, Chem. Eng. Sci. 59 (2004) 6015–6020.
- [21] W. Jamsak, S. Assabumrungrat, P.L. Douglas, N. Laosiripojana, S. Charojrochkul, Chem. Eng. J. 119 (2006) 11–18.
- [22] S.L. Douvartzides, F.A. Coutelieris, A.K. Demin, P.E. Tsiakaras, AIChE J. 49 (2003) 248–257.